Sustained granule cell activity disinhibits juvenile mouse cerebellar stellate cells through presynaptic mechanisms

Simone Astori and Georg Köhr

Department of Molecular Neurobiology, Max-Planck-Institute for Medical Research, Jahnstrasse 29, D-69120 Heidelberg, Germany

GABA release from cerebellar molecular layer interneurons can be modulated by presynaptic glutamate and/or $GABA_B$ receptors upon perfusing the respective agonists. However, it is unclear how release and potential spillover of endogenous transmitter lead to activation of presynaptic receptors. High frequency firing of granule cells, as observed *in vivo* upon sensory stimulation, could lead to glutamate and/or GABA spillover. Here, we established sustained glutamatergic activity in the granule cell layer of acute mouse cerebellar slices and performed 190 paired recordings from connected stellate cells. Train stimulation at 50 Hz reduced by about 30% the peak amplitude of IPSCs evoked by brief depolarization of the presynaptic cell in 2-week-old mice. A presynaptic mechanism was indicated by changes in failure rate, paired-pulse ratio and coefficient of variation of evoked IPSCs. Furthermore, two-photon Ca^{2+} imaging in identified Ca^{2+} hot spots of stellate cell axons confirmed reduced presynaptic Ca^{2+} influx after train stimulation within the granular layer. Pharmacological experiments indicated that glutamate released from parallel fibres activated AMPARs in stellate cells, evoking GABA release from surrounding cells. Consequential GABA spillover activated presynaptic $GABA_B$Rs, which reduced the amplitude of eIPSCs. Two-thirds of the total disinhibitory effect were mediated by $GABA_B$Rs, one-third being attributable to presynaptic AMPARs. This estimation was confirmed by the observation that bath applied baclofen induced a more pronounced reduction of evoked IPSCs than kainate. Granule cell-mediated disinhibition persisted at near-physiological temperature but was strongly diminished in 3-week-old mice. At this age, GABA release probability was not reduced and presynaptic $GABA_B$Rs were still detectable, but GABA uptake appeared to be advanced, attenuating GABA spillover. Thus, sustained granule cell activity modulates stellate cell-to-stellate cell synapses, involving transmitter spillover during a developmentally restricted period.

(Resubmitted 11 October 2007; accepted after revision 14 November 2007; first published online 22 November 2007)
Corresponding author G. Köhr: Department of Molecular Neurobiology, Max-Planck-Institute for Medical Research, Jahnstrasse 29, D-69120 Heidelberg, Germany. Email: kohr@mpimf-heidelberg.mpg.de

The basic neural circuits in the cerebellum are well characterized. Purkinje cells are the only output cells of the cerebellar cortex and receive sensory information from parallel fibres (PF) and climbing fibre (CF) glutamatergic synapses. These excitatory inputs are balanced by the inhibition provided by basket and stellate cells, which are commonly considered as two distinct types of GABAergic interneurons. They are differentially localized in the inner and outer molecular layer, and innervate the somata and the dendrites of Purkinje cells, respectively.

GABAergic synapses of cerebellar interneurons are a component of a feed-forward inhibitory circuit, and earlier studies clearly demonstrated that presynaptic receptors regulate GABA release. Glutamate via AMPARs or NMDARs increases the frequency of miniature IPSCs (mIPSCs) (Bureau & Mulle, 1998; Glitsch & Marty, 1999), whereas GABA via $GABA_B$Rs decreases the frequency of mIPSCs (Mann-Metzer & Yarom, 2002). The temporal role of these effects was mainly studied using the paired-pulse protocol and indicated short-term reductions of evoked IPSCs (eIPSCs) (Glitsch & Marty, 1999; Satake *et al.* 2000; Mann-Metzer & Yarom, 2002), whereas autaptic GABAergic currents in stellate cells can be short- or long-term modulated by AMPARs and NMDARs, respectively (Liu & Lachamp, 2006; Liu, 2007). The molecular mechanism underlying the short-term effects has also been addressed at individual GABAergic synapses, mainly at basket cells. A 10 or 50 Hz stimulation of the CF reduced eIPSCs recorded in Purkinje cells via presynaptic AMPARs (Satake *et al.* 2000, 2004; Rusakov *et al.* 2005). This protocol is likely to induce glutamate spillover in a region restricted to the soma and/or to

 DOI: 10.1113/jphysiol.2007.146522

the most proximal dendritic domain of the Purkinje cell. Equivalent PF-conditioning failed in modulating basket cell-to-Purkinje cell synapses (Satake *et al.* 2000). The presynaptic AMPARs activated by CF-conditioning were supposed to initiate metabotropic functions, whereas involvement of presynaptic $GABA_BRs$ has been excluded (Satake *et al.* 2004).

Here, we investigated how GABAergic transmission between cerebellar stellate cells can be affected by high frequency firing of granule cells, which was observed during sensory activation *in vivo* (Chadderton *et al.* 2004). Unitary connections between stellate cells were studied using whole-cell paired recordings during postnatal development (P13–P22). Fifty hertz stimulation in the granule cell layer caused GABA spillover from molecular layer interneurons, leading to disinhibition at stellate cell-to-stellate cell synapses preferentially in 2-week-old mice. This effect mainly involves presynaptic $GABA_BRs$ on stellate cells and resembles a form of heterosynaptic depression which also exists at PF-to-Purkinje cell synapses and is induced by GABA spillover from interneurons (Dittman & Regehr, 1997). Postsynaptic AMPARs in stellate cells trigger the disynaptic pathway leading to GABA spillover, whereas presynaptic AMPARs contribute to a minor extent in our experimental condition.

Thus, PF and CF conditioning cause disinhibition via distinct mechanisms at presynaptic terminals of stellate cells and basket cells.

Methods

Slice preparation

Sagittal cerebellar slices (250 μm thick) were obtained from 2-week-old (P13–15) and 3-week-old (P19–22) C57Bl/6 mice anaesthetized with halothane or isoflurane and decapitated. All experimental procedures were in accordance with the animal welfare guidelines of the Max Planck Society. The slicing chamber contained an oxygenated ice-cold solution (modified from Dugue *et al.* 2005) composed of (mM): 140 potassium gluconate, 10 Hepes, 15 sodium gluconate, 0.2 EGTA, 4 NaCl (pH 7.2). Slices were incubated for 30 min at 35° before recording in artificial CSF (ACSF) containing (mM): 125 NaCl, 25 $NaHCO_3$, 2.5 KCl, 1.25 NaH_2PO_4, 1 $MgCl_2$, 2 $CaCl_2$, 25 glucose, bubbled with 95% O_2–5% CO_2.

Electrophysiology

Patch pipettes were pulled from borosilicate glass capillaries and had resistances of 5–8 MΩ when filled with (mM): 130 potassium gluconate, 10 Hepes, 10 Phosphocreatine, 10 sodium gluconate, 4 MgATP, 0.3 GTP, 0.2 EGTA, 4 NaCl (pH 7.2). For the postsynaptic cell QX-314CL (2.5 mM) was added to the intracellular solution to block voltage gated Na^+ channels. Slices were constantly perfused with oxygenated ACSF at room temperature, except where indicated. In paired recordings with pharmacological tools, the drugs were continuously present in the extracellular medium, except for the AMPAR antagonist GYKI-53655 and the GAT-1 (GABA transporter) blocker NO-711. GYKI-53655 and NO-711 were added to ACSF and perfused by a peristaltic pump after the extracellular stimulation in the granule cell layer was established. For experiments with the high affinity $GABA_BR$ blocker at low concentration, slices were preincubated in 0.5 μM CGP-55845A. To improve stability of prolonged recordings, 5–10 mM GABA was added to the patch pipette (Figs 4*B* and *C* and 5*B*). This approach had been successfully applied before to maintain sufficient glutamate release in paired recordings (Biro & Nusser, 2005). Experiments using DL-threo-β-benzyloxyaspartate (DL-TBOA) to block glutamate uptake were performed in the presence of 50 μM D-APV to avoid activation of extrasynaptic NMDARs (Clark & Cull-Candy, 2002). For experiments with exogenous agonists, drugs were added to ACSF and perfused by a peristaltic pump.

Unitary connections between stellate cells were found by correlating synaptic responses in an interneuron voltage-clamped at −35/−40 mV with the firing of a putative presynaptic cell monitored in loose cell-attached configuration (Kondo & Marty, 1998). In case of correlation, the presynaptic cell was re-patched in whole-cell configuration and voltage-clamped at −60 mV. Train stimulation was generated in the granule cell layer with an extracellular pipette filled with ACSF. The stimulation strength was adjusted to produce reproducible sub-threshold eEPSCs in the stellate cells upon a train of stimuli. This prevented firing of the presynaptic cell during train stimulation which could induce homosynaptic depression (Glitsch & Marty, 1999; Satake *et al.* 2000; Mann-Metzer & Yarom, 2002). To circumvent the problem of synaptic rundown (Diana & Marty, 2003), the stimulation protocol was kept shorter than 20 min, and test and conditioned responses were carried out in the same stimulation series, so that potential rundown would affect both responses in parallel. Furthermore, the last series of the recorded responses were discarded from the analysis if test responses were reduced more than 50%. The stimulation series was repeated at least 15 times and consisted of three steps: (1) test responses in a paired-pulse protocol (20 ms interval) were evoked in the postsynaptic cell by voltage pulses to the presynaptic cell (0.5–1 ms from −60 mV to 0 mV); (2) after 10 s, a train stimulation at 50 Hz was generated in the granule cell layer; (3) after 40 ms, paired-pulse conditioned responses were evoked in the stellate cell pair. A new stimulation series was started after 20 s to ensure full recovery of test responses. The same protocol was used for studying the $GABA_BR$-mediated

effect in the presence of 50 μM GYKI-53655 (Fig. 4*A*), in these experiments the train stimulation was generated in the molecular layer with an electrode placed within 50 μm from the recorded cells. Stimulus intensity was carefully adjusted to elicit reproducible eIPSCs without inducing presynaptic firing by direct electrical stimulation.

Recordings of spontaneous spikes were performed by patching stellate cells in cell-attached configuration with a pipette filled with ACSF. Due to the difficulty to keep this configuration stable for > 20 min, the pipette was retracted after recording control traces, and the cells were re-patched twice to record firing activity, 10 min after start of NO-711 perfusion and 15 min after wash-out of the blocker. In each condition, traces were recorded for 3 min, and spikes were identified by visual inspection. For estimation of tail current, pharmacologically isolated eIPSCs were evoked in stellate cells at −35 mV by extracellular stimulation in the molecular layer in the presence of 50 μM GYKI-53655 and 50 μM D-APV.

Data acquisition and analysis

The current signals were filtered at 3 kHz and digitized at 10 kHz by the on-board A/D converter of the EPC-10 amplifier controlled by Patchmaster (Heka Elektronik, Lambrecht, Germany). For each series, peak amplitudes of eIPSCs were analysed and the numerical values were averaged. Regarding analysis of the paired-pulse ratio, the peak of the second eIPSC was determined relative to the decaying phase of the first eIPSC. The coefficient of variation of the first peak was calculated as $\sqrt{}(\text{variance}_{\text{eIPSC}})/\text{mean}_{\text{eIPSC}}$. Since agonist perfusion (baclofen, kainate; see Fig. 4) increased the background noise, background variance was subtracted:

$$\text{CV} = \sqrt{}(\text{variance}_{\text{eIPSC}} - \text{variance}_{\text{noise}})/\text{mean}_{\text{eIPSC}}$$

$\text{Variance}_{\text{noise}}$ was determined within a window of 5 ms before the eIPSC. Miniature events were detected and analysed using a macro written for Igor (WaveMetrics, Inc., Lake Oswego, OR, USA). The detection threshold was set at 4–5 pA. For estimation of tail current, average responses in the presence of 5 μM NO-711 were normalized to average responses without GAT-1 blocker relative to the peak of the fifth stimulation of the 50 Hz train. Percentage tail current was calculated by dividing the eIPSC amplitude after 100 ms by the peak amplitude.

All data are presented as means ± S.E.M. Statistical significance was tested using Student's *t* test or ANOVA with Fisher's LSD *post hoc* test ($^*P < 0.05$; $^{**}P < 0.01$).

Two-photon Ca^{2+} imaging

For Ca^{2+} imaging experiments, 2 mM CaCl was added to the extracellular ACSF to amplify the Ca^{2+} signals, and stellate cells were held in whole-cell mode using the intracellular solution described above supplemented with 100 μM of the K^+ salt of the Ca^{2+} sensitive dye Oregon Green 488 BAPTA-1 (Molecular Probes). A good labelling of the axon was reached after allowing the dye to diffuse into the cell for at least 30 min. The axon was identified by morphology and by functional criteria (presence of 'hot spots', i.e. local maxima in the Ca^{2+} responses, as described in Forti *et al.* 2000). Granule cell axons were labelled by electroporation of the cells with 500 μM Alexa Fluor 594 (Molecular Probes) contained in the stimulation pipette. Parallel fibre trunks were traceable after three to five repetitions of train stimulation, which was performed in the same manner as for double-patch experiments. Two-photon excitation was performed with a mode-locked 170 fs pulse Ti-Sapphire laser (Chameleon XR; Coherent, CA, USA) set at an excitation wavelength of 840 nm. The system used an upright Zeiss microscope equipped with a 63× water immersion objective. Fluorescence signals were acquired with the LSM 510 software (Zeiss, Germany). Frame scan acquisition (150 frames) was performed from regions of interest (ROIs) set on the stellate cell axons in correspondence to hot spots of Ca^{2+} signals. ROIs had a size of 30 × 20 pixels (pixel size 40 nm × 40 nm) and were scanned every 30.27 ms (pixel dwell time = 1.28 μs) resulting in a time resolution of 33 ms. For background signal, a similar frame was scanned in parallel in a nearby region not containing the axon. Four to nine ROIs were recorded per cell.

Test Ca^{2+} transients were acquired upon firing of the cell elicited with paired-pulse voltage steps (from −60 to 0 mV, 0.5–1 ms, 20 ms interval) after a 500 ms baseline. For conditioned Ca^{2+} transients, train stimulation (30 stimuli, 50 Hz) was performed in the granule cell layer after 500 ms baseline and was followed after 40 ms by paired-pulse firing of the cell. Test and conditioned responses were alternatively acquired. To minimize noise, three signals were averaged for each ROI before determining peak transients. ROIs that showed rundown in the test responses, probably induced by photobleaching and/or photodamaging, were not considered. Offline analysis of the fluorescence signals was performed using a macro written for Igor. Values are expressed as the percentage change in fluorescence with respect to baseline:

$$\Delta F/F_0 = 100(F - F_0)/(F_0 - B)$$

where F is the measured fluorescence signal at any given time, F_0 is the average from the prestimulus signal, and B is the value of the background fluorescence.

Drugs

Pharmacological tools were obtained from Tocris (D-APV, CGP-55845A, CGP-35348, AM251, AIDA, S-MCPG, CPPG, DL-TBOA) and from Sigma Aldrich

(GDPβ-S, baclofen, TTX, NO-711, SR-95531, kainate). QX314-Cl was purchased from Alomone Laboratories Ltd (Jerusalem, Israel). Dyes for Ca^{2+} imaging experiments were purchased from Molecular Probes. GYKI-53655 was kindly provided by IVAX Drug Research Institute Ltd (Budapest, Hungary).

Results

Granule cell activity modulates presynaptic Ca^{2+} transients in stellate cells

Neurotransmitter can spill over during high levels of synaptic activity. Following high frequency firing of granule cells, glutamate released from parallel fibres (Carter & Regehr, 2000) and/or GABA released by excited surrounding interneurons (Dittman & Regehr, 1997) could diffuse to axon terminals of stellate cells and activate presynaptic receptors.

To find out whether Ca^{2+} entry into presynaptic terminals of stellate cells is modulated by endogenous neurotransmitter release, we examined Ca^{2+} transients in axons of stellate cells using two-photon Ca^{2+} imaging before and after a train stimulation within the granule cell layer to release glutamate from parallel fibres (axons of granule cells). In acute sagittal slices of 2-week-old mice, stellate cells in the outer two-thirds of the molecular layer were loaded with 100 μM Oregon Green 488 BAPTA-1 (Fig. 1*A*). Ca^{2+} transients in axons were evoked upon firing of the stellate cells, which were voltage clamped, and two spikes were evoked by a 20 ms double pulse protocol (from −60 mV to 0 mV for 0.5–1 ms). We concentrated on 'hot spots' which mostly coincide with axonal varicosities and give rise to *en passant* presynaptic sites (Forti *et al.* 2000). To ensure that glutamate was released in a region proximal to the stellate cell axon, we traced the granule cell axons following electroporation with Alexa Fluor 594 (500 μM), which was present in the extracellular stimulation pipette. Sufficient labelling of the axon was reached after very few train stimulations (30 stimuli at 50 Hz; Fig. 1*A*).

Test Ca^{2+} transients from different 'hot spots' within the same axon (e.g. region of interest (ROI) in Fig. 1*B*) were examined in different cells and were analysed as $\Delta F/F_0$, as described in Methods. The train stimulation itself (30 stimuli at 50 Hz) did not produce a detectable axonal Ca^{2+} signal (Fig. 1*C*), indicating that release of glutamate did not generate a detectable Ca^{2+} influx in the axon through Ca^{2+} permeable AMPARs and/or voltage gated Ca^{2+} channels. Notably, the conditioned Ca^{2+} transients examined 40 ms after the train stimulation were reduced compared with the test Ca^{2+} transients by $11.4 \pm 1.9\%$ ($P < 0.01$, number of ROIs $N = 53$, number of cells $n = 9$; Fig. 1*D*; 'enlarged overlay' in Fig. 1*C*). The kinetics of the Ca^{2+} transients were not significantly changed (rise time 10–90% and decay time from monoexponential fit: 55.7 ± 3.9 ms and 4.0 ± 0.3 s for test responses *versus* 60.9 ± 3.5 ms and 3.9 ± 0.2 s for conditioned responses, $N = 53$, $n = 9$, $P > 0.05$; 'scaled overlay' in Fig. 1*C*). In the presence of the specific AMPAR antagonist GYKI-53655 (50 μM), the conditioned Ca^{2+} transients were not reduced ($0.15 \pm 1.98\%$, $P > 0.05$, $N = 42$, $n = 8$) and were different from control (ANOVA, $P < 0.01$), indicating the involvement of AMPARs. To test whether $GABA_BRs$ are involved, we preincubated the slices with the specific, high affinity $GABA_BR$ antagonist CGP-55845A at 0.5 μM. In the presence of CGP-55845A, conditioned Ca^{2+} transients were affected to some extent but were still reduced by $6.8 \pm 1.6\%$ ($P < 0.01$, $N = 41$, $n = 8$), different from GYKI-53655 (ANOVA, $P < 0.05$).

In summary, in 2-week-old mice action potential-triggered axonal Ca^{2+} transients in stellate cells were reduced following train stimulation in the granule cell layer. This effect was reduced by a $GABA_BR$ antagonist, and it was blocked by an AMPAR antagonist.

Disinhibition at stellate cell-to-stellate cell synapses

A limitation of the above Ca^{2+} imaging approach is that the amount and the spatial extent of glutamate and GABA release during the train stimulation could not be controlled, although the labelling of granule cells' axons with Alexa provided an indication about the proximity of the excitatory inputs to the imaged axon of the stellate cells. In addition, the postsynaptic targets (interneurons or Purkinje cells) of those presynaptic terminals could not be discriminated. Therefore, we next performed double-patch recordings from synaptically connected cerebellar stellate cells. Short voltage pulses to the presynaptic neuron using the 20 ms paired-pulse protocol evoked inhibitory postsynaptic currents (eIPSCs; Fig. 2). These eIPSCs were outward at −35/−40 mV because of a low chloride concentration in the patch pipette (6.5 mM). For a single connection, the paired-pulse ratio was estimated after averaging over many responses (> 15) and was 0.96 ± 0.02, $n = 109$. The average peak amplitudes of eIPSCs in different interneuron pairs ranged between 20 and 200 pA (56.6 ± 3.4 pA, $n = 109$). This variability reflects the presence of single or multiple release sites (Kondo & Marty, 1998).

To find out whether IPSCs evoked in the paired-pulse protocol are also modulated by endogenous glutamate, test eIPSCs were compared with conditioned eIPSCs generated 40 ms after the end of a train stimulation within the granule cell layer using an extracellular pipette (Fig. 2*A*). Thirty stimuli at 50 Hz simultaneously evoked EPSCs and IPSCs via disynaptic activation, which reduced the amplitude of the conditioned eIPSC ($28.0 \pm 4.7\%$ for the first peak, $P < 0.01$ and $19.5 \pm 4.5\%$ for the second peak, $P < 0.05$, $n = 8$; Fig. 2*B*). We continued to use this stimulation protocol throughout the study, since, for

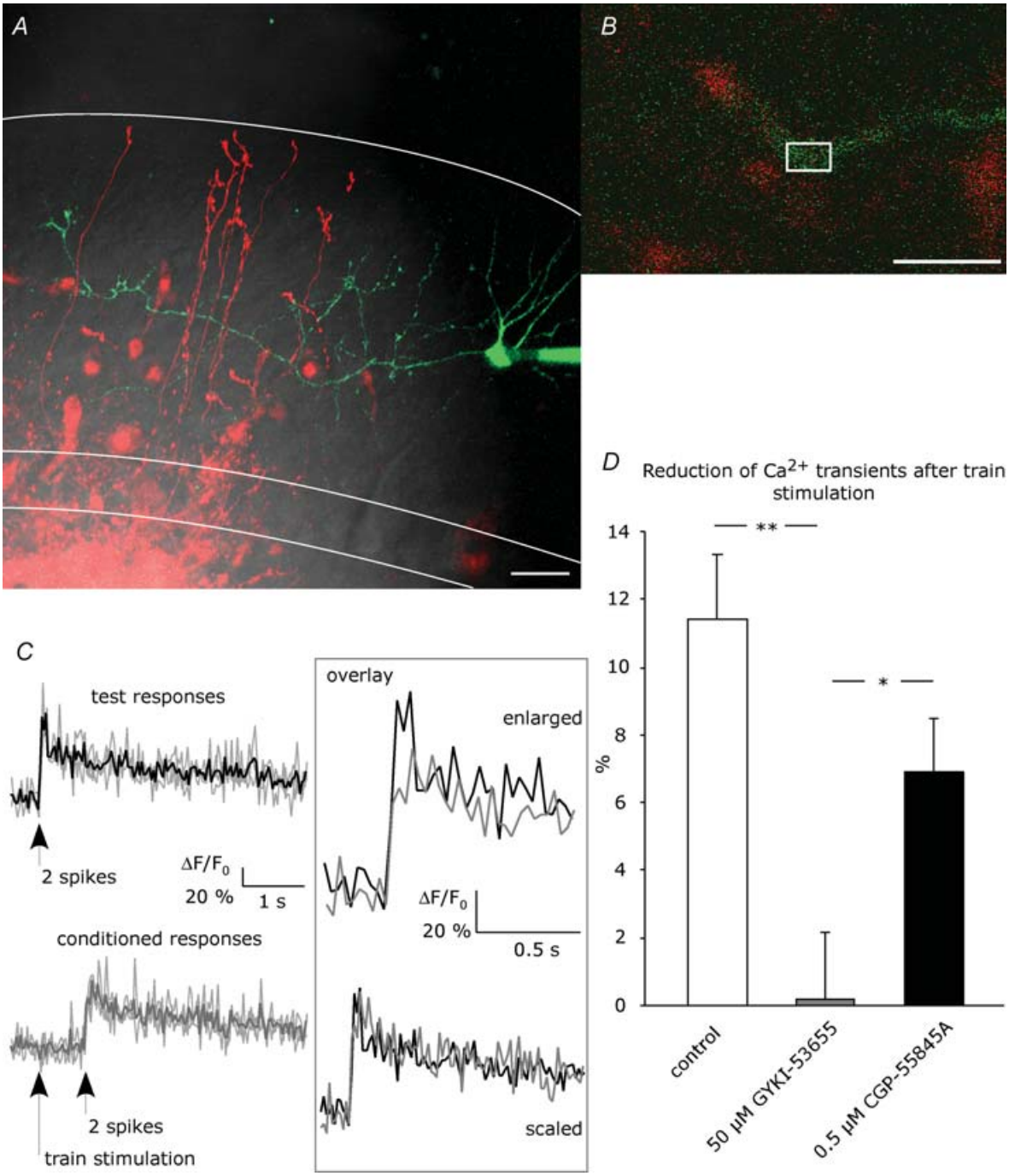

Figure 1. Ca^{2+} imaging in stellate cell axons
A, a stellate cell was loaded with 100 μM Oregon Green 488 BAPTA-1 via the patch pipette. Granule cells were filled by electroporation achieved with repetitive stimulation in the granule cell layer with an extracellular pipette containing 500 μM Alexa Fluor 594. This picture is a z-projection, collecting the maximum intensity from 28 images taken in different focal planes with 1 μm intervals (scale bar = 20 μm). DIC, red and green channels are overlaid. White lines indicate Purkinje cell layer and rim of the molecular layer. Ca^{2+} signals were evoked by paired-pulse spiking of the stellate cells and were measured in ROIs set on the interneuron axon in proximity to granule cell axons, as depicted in an example in *B* (scale bar = 10 μm). *C*, example of test responses (black) and conditioned responses (grey) from a single hot spot. Fluorescence signals from 3 trials (depicted by faint lines) were analysed as $\Delta F/F_0$ and averaged. No Ca^{2+} signals were detected upon train stimulation. Scaling of the average traces revealed no change in the kinetics. *D*, reduction of peak amplitude of conditioned Ca^{2+} transients compared to test transients was examined in the absence of drug (control; number of ROIs, $N = 53$) and in the presence of AMPAR blocker (50 μM GYKI-53655, $N = 42$) or $GABA_BR$ blocker (0.5 μM CGP-55845A, $N = 41$). Asterisks indicate statistical significance among series tested using ANOVA with Fisher's LSD *post hoc* test ($^*P < 0.05$; $^{**}P < 0.01$).

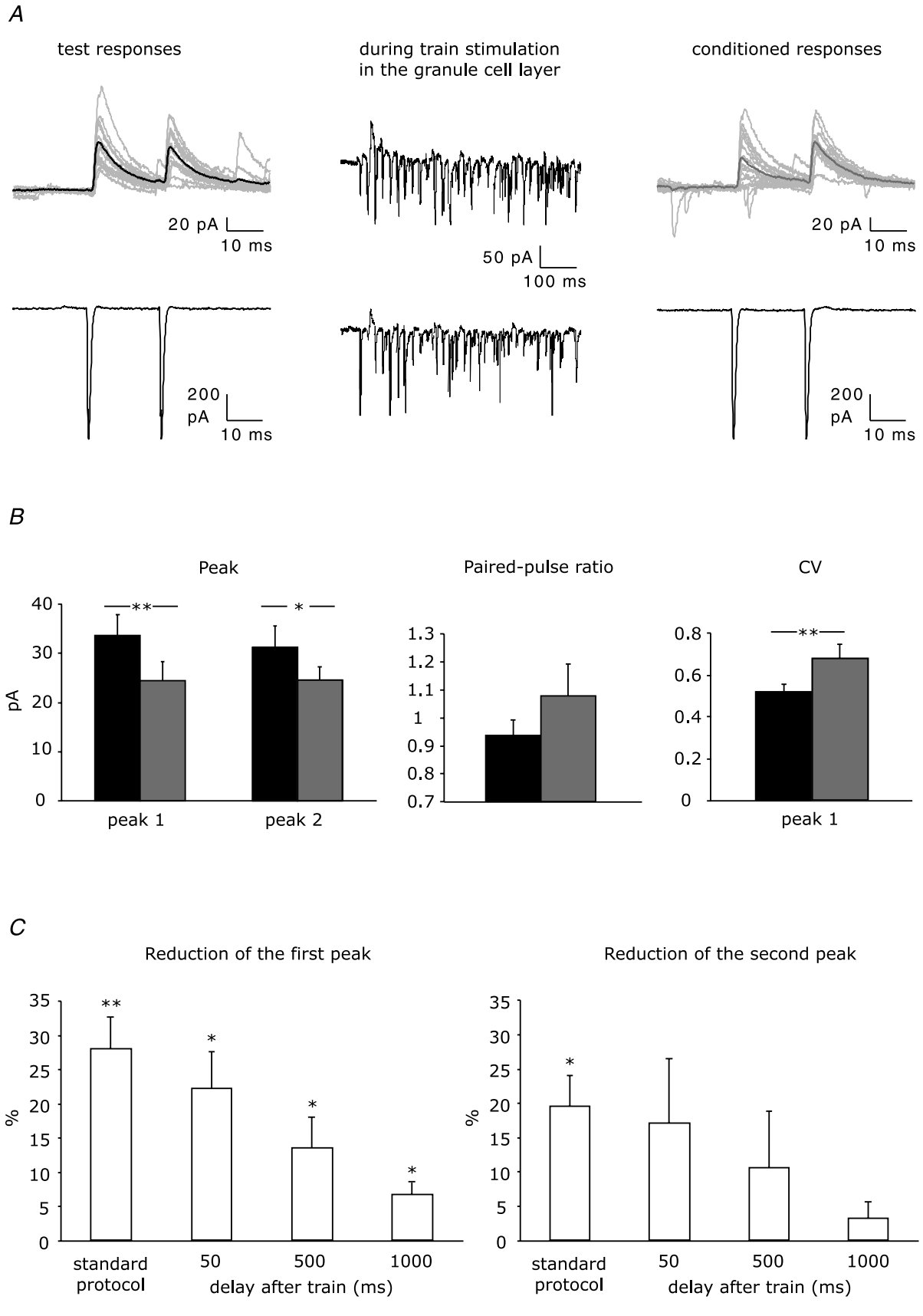

example, 60 stimuli at 50 Hz were less efficient than 30 stimuli (17.6 ± 4.7% reduction of the first peak, $P < 0.05$, $n = 10$; not illustrated). The conditioned eIPSCs were reduced in an activity-dependent manner and were not reduced due to synaptic rundown (e.g. Diana & Marty, 2003), since both test and conditioned eIPSCs were carried out in the same series (see Methods for further details).

Concomitant with the peak amplitude reduction (see above), the failure rate in the conditioned eIPSCs could increase at both peaks in the paired-pulse response (18.5 ± 5.7% for the first and 18.0 ± 3.5% for the second peak of conditioned eIPSCs, compared to 6.3 ± 2.9% and 8.0 ± 4.2% in test eIPSCs; $P < 0.05$, $n = 8$) and the paired-pulse ratio shifted towards paired-pulse facilitation (from 0.94 ± 0.05 to 1.08 ± 0.11; $P > 0.05$, $n = 8$; Fig. 2*B*). These changes in failure rate and paired-pulse ratio strongly suggested a presynaptic mechanism, i.e. reduced GABA release, which was supported by an increase in the coefficient of variation of the eIPSC amplitude (CV = s.d. × mean amplitude^{-1}). CV of the first peak increased from 0.52 ± 0.04 in test eIPSCs to 0.68 ± 0.07 in conditioned eIPSCs ($P < 0.01$, $n = 8$; Fig. 2*B*). Together, release of endogenous glutamate from granule cells weakens the inhibitory input to stellate cells and thus disinhibits the stellate cell network via presynaptic mechanisms.

Next, we investigated the influence of the time delay between train stimulation and conditioned eIPSCs for the disinhibition at stellate cell-to-stellate cell synapses. For this, additional 50, 500 or 1000 ms were inserted between train and conditioned eIPSCs which were separated by 40 ms in the standard protocol (Fig. 2*C*). With increasing delay, the reduction of the first peak of the conditioned eIPSCs became less pronounced but remained significant even with a delay of 1000 ms (50 ms, 22.3 ± 5.4%, $n = 6$; 500 ms, 13.6 ± 4.5%, $n = 7$; 1000 ms, 6.7 ± 1.8%, $n = 6$; $P < 0.05$ in all cases). The second peak of the conditioned eIPSC was no longer significantly reduced when the delay was prolonged by 50, 500 or 1000 ms (17.0 ± 9.5%, $n = 6$; 10.6 ± 8.2%, $n = 7$ or 3.2 ± 2.2%, $n = 6$; $P > 0.05$ in all cases).

Thus, disinhibition at stellate cell-to-stellate cell synapses involves presynaptic mechanisms which are activated within tens of milliseconds and last as long as 1 s.

Pharmacological dissection of disinhibition at stellate cell-to-stellate cell synapses

Glutamate released by the train stimulation in the granule cell layer was expected to activate glutamate receptors. To find out which of the ionotropic GluRs were involved in modulating GABA release, we performed experiments in the presence of either AMPAR or NMDAR antagonists and compared the effects on the conditioned eIPSCs with the reduction observed in absence of drug (see above). As expected from the two-photon Ca^{2+} imaging experiments, presence of the AMPAR antagonist GYKI-53655 (50 μM) prevented a reduction of the eIPSCs (e.g. first peak, 5.1 ± 3.5%, $P > 0.05$, $n = 8$; Fig. 3*A*). This result confirms that AMPARs were involved in disinhibiting stellate cells. In contrast, in the presence of the specific NMDAR antagonist D-APV (50 μM), the conditioned eIPSCs were reduced as in the control experiment (24.9 ± 4.9%, $P < 0.05$, $n = 7$), ruling out the involvement of NMDARs. This was confirmed by an opposite approach in which NMDAR activation was favoured by lowering the extracellular magnesium concentration (0.1 mM instead of 1 mM), which did not result in a stronger reduction of the conditioned eIPSCs than in control (26.4 ± 4.9%, $P < 0.05$, $n = 8$).

To examine the involvement of $GABA_B$Rs (Mann-Metzer & Yarom, 2002), which could become activated by GABA released from stellate cells when activated by postsynaptic AMPARs, we used the low affinity $GABA_B$R antagonist CGP-35348 at high concentrations (100 μM) and obtained quite variable effects. Either the conditioned eIPSCs were reduced as in the control experiment (23.3 ± 6.6%, $P = 0.06$, $n = 3$) or the conditioned responses were potentiated (−24.4 ± 5.5%, $P < 0.005$, $n = 3$). Although on average CGP-35348 completely prevented a reduction of the eIPSCs (−0.5 ± 11.3%, $P > 0.05$, $n = 6$), this result remained unclear. Next, we tested the high affinity $GABA_B$R antagonist CGP-55845A, which was preincubated for 20–30 min at 0.5 μM. CGP-55845A did not prevent a reduction of

Figure 2. Disinhibition at unitary connections between stellate cells
A, example traces from a paired recording. The postsynaptic (upper panel) and presynaptic cell (lower panel) were voltage-clamped at −35 mV and −60 mV, respectively. Test and conditioned IPSCs in the postsynaptic cell were evoked by firing elicited in the presynaptic cell by paired depolarization pulses. Conditioned eIPSCs were preceded by train stimulation in the granule cell layer. Average of 15 test and 15 conditioned eIPSCs is shown by a thick line in black and grey, respectively. *B*, effect of a train of 30 stimuli in the granule cell layer on peak amplitude, paired-pulse ratio and CV of eIPSCs in stellate cell pairs ($n = 8$). Test and conditioned responses are indicated by black and grey bars, respectively. *C*, reduction of amplitude of first and second peak of paired-pulse eIPSCs using standard protocol (40 ms between the end of train stimulation and the conditioned responses, $n = 8$) and protocols in which a further delay of 50, 500 or 1000 ms was added after the train ($n = 6$, $n = 7$, $n = 6$, respectively). Asterisks indicate statistical significance tested with paired Student's *t* test (test responses *versus* conditioned responses, $^{*}P < 0.05$; $^{**}P < 0.01$).

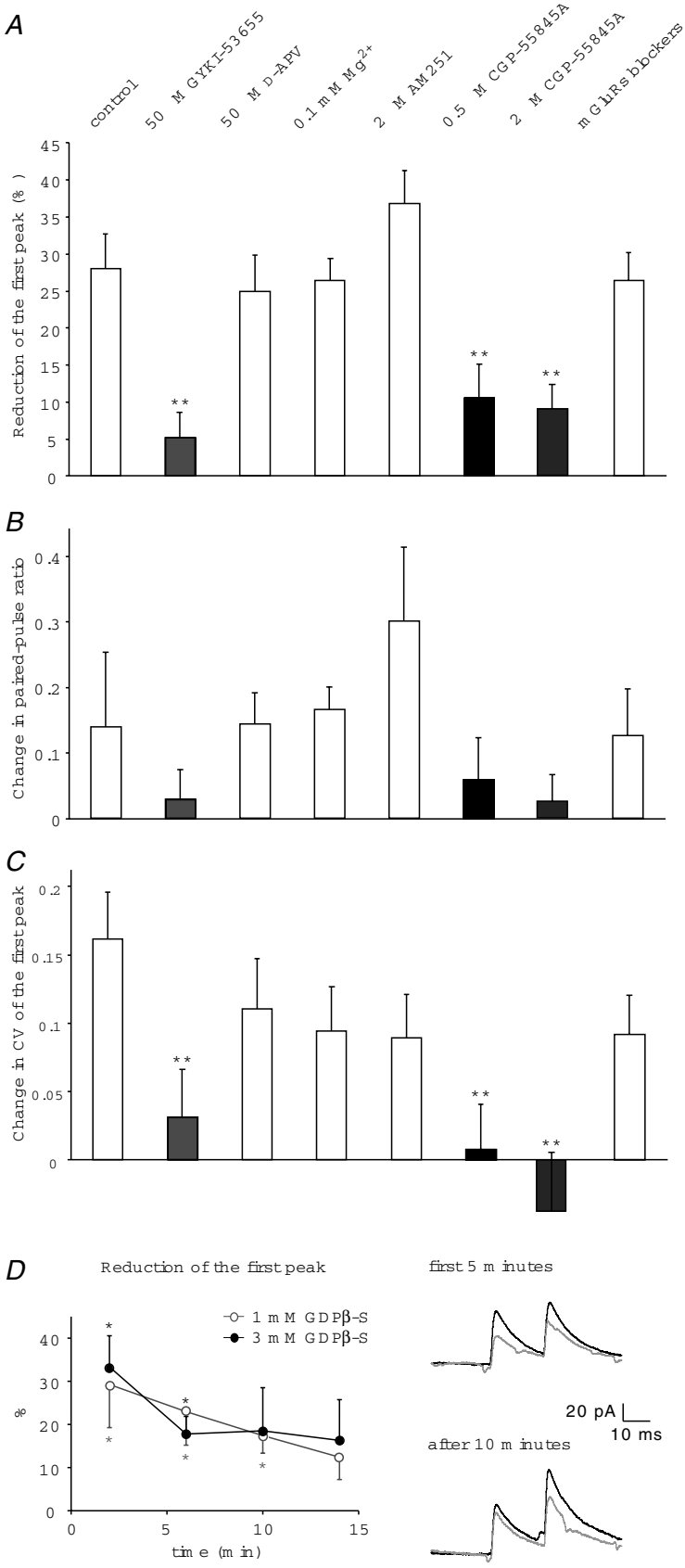

Figure 3. Pharmacological dissection of the disinhibitory effect
A, reduction of conditioned eIPSCs (first peak of paired-pulse) in different experimental conditions: control ($n = 8$), AMPAR blocker (50 μM GYKI-53655, $n = 8$), NMDAR blocker (50 μM D-APV, $n = 7$), 0.1 mM extracellular Mg^{2+} ($n = 8$), CB1 receptor blocker (2 μM AM251, $n = 6$), $GABA_BR$ blockers (0.5 μM and 2 μM CGP-55845A, $n = 8$ and $n = 6$, respectively) and mGluR blockers (300 μM AIDA, 500 μM S-MCPG, 500 μM CPPG, $n = 11$). *B* and *C*, changes in paired-pulse ratio and CV of the first peak were calculated as difference between the values for the conditioned responses and the values for test responses. Statistical significance in comparison to control experiment was tested using ANOVA with Fisher's LSD *post hoc* test ($^*P < 0.05$; $^{**}P < 0.01$). *D*, G proteins in the presynaptic cell were blocked by including GDPβ-S in the patch pipette at two different concentrations (1 mM, e, $n = 8$; 3 mM, ●, $n = 6$). On the left, reduction of eIPSCs is plotted against the time of presynaptic whole-cell. Each data point corresponds to the average of 8 responses. On the right, example traces from a single recording with 1 mM GDPβ-S: average test responses (black) and conditioned responses (grey) at the beginning and after 10 min of recording. See Fig. 2*C* for statistical significance.

the conditioned eIPSCs ($10.5 \pm 4.6\%$, $P < 0.05$, $n = 8$; Fig. 3*A*), but the remaining effect was smaller than in absence of drug (ANOVA, $P < 0.01$). Even at 2 μM, a concentration sufficient to antagonize baclofen effects on mIPSCs (see below), CGP-55845A did not prevent the reduction of the conditioned eIPSCs ($9.0 \pm 3.2\%$, $P = 0.06$, $n = 6$; Fig. 3*A*), similarly to CGP-55845A at 0.5 μM. This indicates that the activation of presynaptic $GABA_B$Rs could be the second step of a disynaptic pathway initiated by glutamate release which disinhibits stellate cell-to-stellate cell synapses.

We could not find evidence for an involvement of metabotropic GluRs (mGluRs) or endocannabinoids. Endocannabinoids play an important role in modulating synaptic transmission in the cerebellar network (Diana & Bregestovski, 2005) and were probably liberated in response to the depolarization mediated by glutamate released during the train. However, the CB1 receptor antagonist AM251 (2 μM) had no effect on the disinhibition ($36.7 \pm 4.5\%$, $P < 0.01$, $n = 6$; Fig. 3*A*) excluding a contribution of endocannabinoids. In addition, mGluRs were not involved, since a cocktail of drugs containing 300 μM AIDA, 500 μM S-MCPG and 500 μM CPPG, which antagonize unselectively group I, group I/II and group II/III mGluRs, respectively, still allowed significant reduction of the conditioned eIPSCs by $26.4 \pm 3.8\%$ ($P < 0.01$, $n = 11$).

The analysis of paired-pulse ratio and CV from all pharmacological experiments (Fig. 3*B* and *C*) confirmed that the disinhibitory effect is because of a presynaptic modulation in GABA release. Limiting the reduction of the conditioned eIPSCs, by either an AMPAR antagonist or by CGP-55845A, diminished changes of the paired-pulse ratio and precluded CV changes. In contrast, paired-pulse ratio and CV changed in the presence of all other antagonists similarly to the control experiment. To provide further evidence that GABA release is modulated by presynaptic $GABA_B$Rs, we took advantage of the fact that $GABA_B$Rs act via G proteins. To impair the function of $GABA_B$Rs exclusively in the presynaptic cell, we included GDPβ-S instead of GTP in the patch pipette. GDPβ-S was employed at two different concentrations (1 and 3 mM) to permit different diffusion efficiencies into the cytoplasm. With 1 mM GDPβ-S, 30 stimuli at 50 Hz caused significant disinhibition at the beginning of the whole-cell recording ($29.1 \pm 9.9\%$, $P < 0.05$, $n = 8$) but no longer 14 min later ($12.3 \pm 5.2\%$, $P > 0.05$, $n = 8$; Fig. 3*D*). With 3 mM GDPβ-S, a pronounced reduction of disinhibition was reached within a shorter time, after about 6 min, and disinhibition was no longer significant at 10 min ($18.5 \pm 10.0\%$, $P > 0.05$ *versus* $33.3 \pm 7.3\%$, $P < 0.05$, observed at the beginning, $n = 6$; Fig. 3*D*). Notably, disinhibition remained significant when 3 mM GDPβ-S was present in the postsynaptic cell ($19.0 \pm 4.2\%$, $P < 0.05$, at 10 min *versus* $26.0 \pm 5.2\%$, $P < 0.05$, observed at the beginning, $n = 5$), indicating that postsynaptic $GABA_B$Rs are unlikely to be involved.

In summary, high levels of activity of granule cells mainly led to activation of presynaptic $GABA_B$Rs in stellate cells, which reduced GABA release via G proteins. This disinhibition is heterosynaptic, since it involved GABA spillover from surrounding interneurons which were activated during train stimulation by postsynaptic AMPARs. Consistently, AMPAR blockade completely prevented disinhibition.

Isolating $GABA_B$R- and AMPAR-mediated disinhibition

Granule cell-mediated disinhibition is heterosynaptic, involving presynaptic $GABA_B$R but potentially also presynaptic AMPARs, since the remaining disinhibitory effect in the presence of the high affinity $GABA_B$R antagonist CGP-55845A (0.5 and 2 μM) and in the presence of GDPβ-S in the presynaptic neuron could be caused by presynaptic AMPARs (Liu, 2007). Though the granule cell-mediated conditioning represents a physiologically relevant protocol, this protocol cannot clearly separate the AMPAR- from the $GABA_B$R-mediated component of the disinhibition. These two concurring pathways are indeed affected by many variables, which might be different for each paired recording, e.g. the amount of glutamate and GABA spillover generated by the train stimulation and/or the density of the two presynaptic receptor types.

As a first attempt to examine $GABA_B$R activation in isolation from AMPAR activation, we recorded from synaptically coupled stellate cells in the presence of 50 μM GYKI-53655 and performed the conditioning train by stimulating surrounding stellate cells in the molecular layer. The amplitude of eIPSC was reduced by $19.1 \pm 3.0\%$ ($P < 0.05$, $n = 6$; Fig. 4*A*), and this effect was confirmed to be mediated by $GABA_B$Rs, since it was completely blocked in the presence of 2 μM CGP-55845A ($3.7 \pm 5.7\%$, $P > 0.05$, $n = 6$). Despite the significant level of disinhibition induced by molecular layer stimulation, neither PPR nor CV showed the expected changes (PPR, from 0.81 ± 0.05 to 0.85 ± 0.08, $P > 0.05$, $n = 6$; CV, from 0.36 ± 0.02 to 0.36 ± 0.03, $P > 0.05$, $n = 6$). This was quite surprising, since the same population of presynaptic $GABA_B$Rs can be assumed to become activated by spillover of GABA, regardless of whether surrounding interneurons are activated by direct electrical stimulation in the molecular layer or via granule cell excitation. An involvement of postsynaptic $GABA_B$Rs in the cell pair under investigation can be excluded, since postsynaptic $GABA_B$Rs have been shown to reduce spiking frequency of stellate cells, whereas modulation of GABA release has been ascribed to presynaptic $GABA_B$Rs (Mann-Metzer & Yarom, 2002). We therefore considered that a change of presynaptic

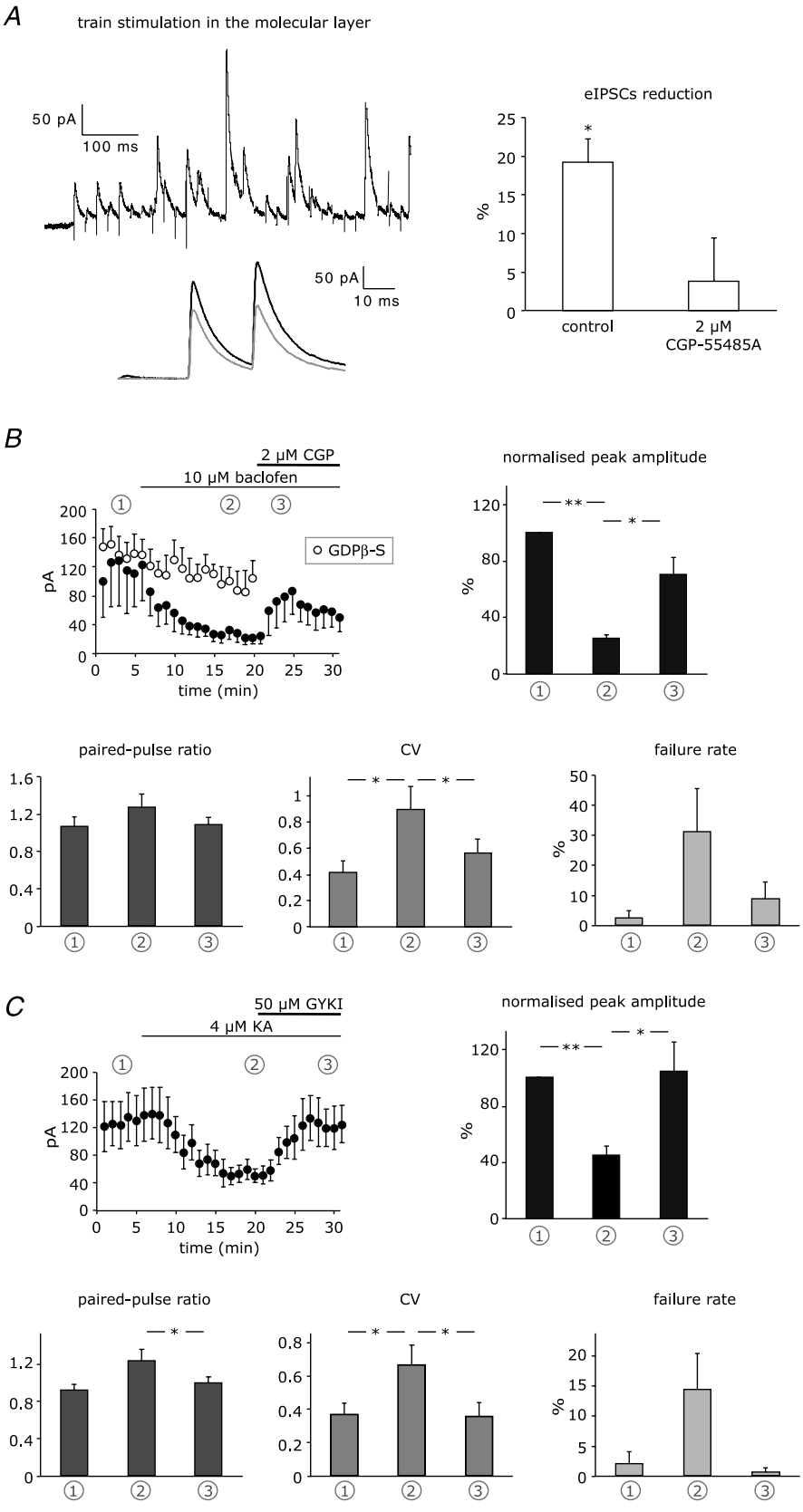

parameters might be verified only in the presence of a more pronounced disinhibitory effect (as observed for granule cell-mediated disinhibition), and that this could be achieved by application of exogenous agonists. Although this method is not comparable to a physiological protocol, it allows a clear pharmacological dissection of the $GABA_BR$- and AMPAR-mediated pathways.

To isolate $GABA_BR$-induced effects, we superfused 10 μM baclofen while evoking IPSCs in stellate cell pairs in the presence of GYKI-53655. The amplitude of eIPSCs was strongly reduced by $74.8 \pm 2.4\%$ ($P < 0.001$, $n = 5$; Fig. 4*B*) and substantially recovered after perfusion of 2 μM CGP-55845A ($P < 0.05$). Notably, PPR, CV and failure rate reversibly increased, confirming the involvement of presynaptic $GABA_BRs$ (PPR, from 1.06 ± 0.11 to 1.27 ± 0.14, $P > 0.05$; CV, from 0.41 ± 0.09 to 0.90 ± 0.18, $P < 0.05$; failure rate, from $2.4 \pm 2.4\%$ to $31.2 \pm 14.4\%$, $P = 0.09$; Fig. 4*B*). Furthermore, blockade of presynaptic G-proteins by 3 mM GDPβ-S prevented the baclofen effect on eIPSC peak (Fig. 4*B*). After 15 min baclofen perfusion, eIPSC peaks were reduced to only $77.7 \pm 8.8\%$ compared to control ($n = 4$), similarly to eIPSCs recovered with CGP-55845A ($70.6 \pm 11.7\%$, $n = 5$).

To isolate AMPAR-induced effects, we superfused 4 μM kainate while evoking IPSCs in stellate cell pairs in the presence of 2 μM CGP-55845A, which decreased eIPSC amplitude by $54.7 \pm 6.2\%$ ($P < 0.001$, $n = 6$; Fig. 4*C*), as expected (Liu, 2007). This reduction was about twice the reduction observed during paired recordings involving AMPARs and $GABA_BRs$ (see above) and was completely reversed by 50 μM GYKI-53655. The involved AMPARs were presynaptic, as indicated by the simultaneous reversible increases of PPR, CV and failure rate (PPR, from 0.92 ± 0.05 to 1.23 ± 0.12, $P < 0.05$, $n = 6$; CV, from 0.37 ± 0.07 to 0.67 ± 0.12, $P < 0.05$, $n = 6$; failure rate, from $2.0 \pm 2.0\%$ to $14.3 \pm 6.1\%$, $P = 0.07$; Fig. 4*C*).

In summary, experiments with exogenous agonists unequivocally demonstrate that both presynaptic $GABA_BRs$ and presynaptic AMPARs are capable of mediating disinhibition. Interestingly, the maximal disinhibitory effect evoked by baclofen was much larger than the kainate induced disinhibition (*ca* 75% *versus* 55% reduction of eIPSCs). This substantiates our main finding that spillover-induced disinhibition was mainly mediated by $GABA_BRs$ (Fig. 3).

Influence of transmitter spillover

Heterosynaptic depression in stellate cell-to-stellate cell synapses via presynaptic receptors requires transmitter spillover. In rat cerebellar slices, parallel fibre activation by brief stimulus trains causes glutamate spillover (Carter & Regehr, 2000) and, because of the activation of molecular layer interneurons, GABA spillover (Dittman & Regehr, 1997). Also the train stimulation in the granule cell layer as performed above, e.g. 30 stimulations in Fig. 2*A*, released glutamate and in addition activated many stellate cells which simultaneously released GABA. The extent of glutamate and GABA spillover is controlled by temperature sensitive uptake systems. To find out whether higher temperature reduces transmitter spillover and consequently the disinhibitory effect, we performed experiments at near-physiological temperature (34°C) to prove physiological relevance. Although paired recordings were less stable and shorter lasting at 34°C, disinhibition was still significant ($20.0 \pm 5.1\%$, $P < 0.05$, $n = 8$) but it was reduced to some extent when compared to room temperature ($28.0 \pm 4.7\%$, $P < 0.01$, $n = 8$).

Blockade of transmitter uptake systems should enhance transmitter spillover, thereby increasing the disinhibitory effect. To be able to examine the consequences of glutamate or GABA uptake blockade for prolonged periods, we performed experiments at room temperature. First, we inhibited the glutamate transporters with 50 μM DL-TBOA. Inhibition of the glutamate uptake system was indicated by the prolonged AMPAR-mediated eEPSCs (Fig. 5*A*), but the extent of disinhibition did not increase in the presence of DL-TBOA ($25.1 \pm 7.6\%$, $P < 0.05$, $n = 8$; Fig. 5*A*). This supports the above conclusion

Figure 4. Isolation of $GABA_BR$ and AMPAR-mediated effects
A, paired recordings were performed in the presence of 50 μM GYKI-53655 and conditioning trains of IPSCs were evoked by extracellular stimulation in the molecular layer, as shown in the example trace on the left. Conditioned responses (grey) were reduced in comparison to test eIPSCs (black). Disinhibition was mediated by $GABA_BRs$, as shown in the bars on the right (control, $n = 6$; 2 μM CGP-55845A, $n = 6$). See Fig. 2*C* for statistical significance. *B*, eIPSCs from paired recordings in the presence of 50 μM GYKI-53655 were reduced upon superfusion of 10 μM baclofen and substantially recovered after $GABA_BR$ blockade with 2 μM CGP-55845A, as shown in the peak amplitude plot on the left (●, $n = 5$). Blockade of G proteins in the presynaptic cell blocked by infusion of 3 mM GDPβ-S prevented significant changes in peak amplitude (ᵉ, $n = 4$). Each data point corresponds to the average of 6 responses. Bar graphs show the reversible changes in peak amplitude, paired-pulse ratio, coefficient of variation and failure rate of the first peak, as measured at different time points: average of 5 min during control (1), agonist perfusion (2), and blocker perfusion (3). *C*, eIPSCs from paired recordings in the presence of 2 μM CGP-55845A were reduced upon superfusion of 4 μM kainate and completely recovered after AMPAR blockade with 50 μM GYKI-53655 ($n = 6$). For bar graphs, see *B*. Asterisks indicate statistical significance tested with paired Student's *t* test.

that the disynaptic pathway which disinhibits stellate cell-to-stellate cell synapses uses glutamate mainly during its first step to activate the stellate cells.

Next, we blocked the GABA transporter GAT-1, which controls the reuptake of GABA into the presynaptic terminals of molecular layer interneurons (Takayama & Inoue, 2005). At the beginning of the GAT-1 blocker perfusion (NO-711, 5 μM), the disinhibitory effect was more robust than in control experiments ($41.3 \pm 8.2\%$, $P < 0.01$, $n = 6$ *versus* $28.0 \pm 4.7\%$, $P < 0.01$, $n = 8$; Fig. 5*B*), indicating that more presynaptic $GABA_B$Rs were activated when GABA uptake was blocked. However, about 20 min after starting drug perfusion, disinhibition was no longer significant ($13.3 \pm 9.7\%$, $P > 0.05$). During the train stimulation, we noticed in some cases a pronounced reduction of the IPSC but not EPSC fraction (see example traces in Fig. 5*B*). To find out whether the enhanced GABA concentration because of GABA uptake blockade

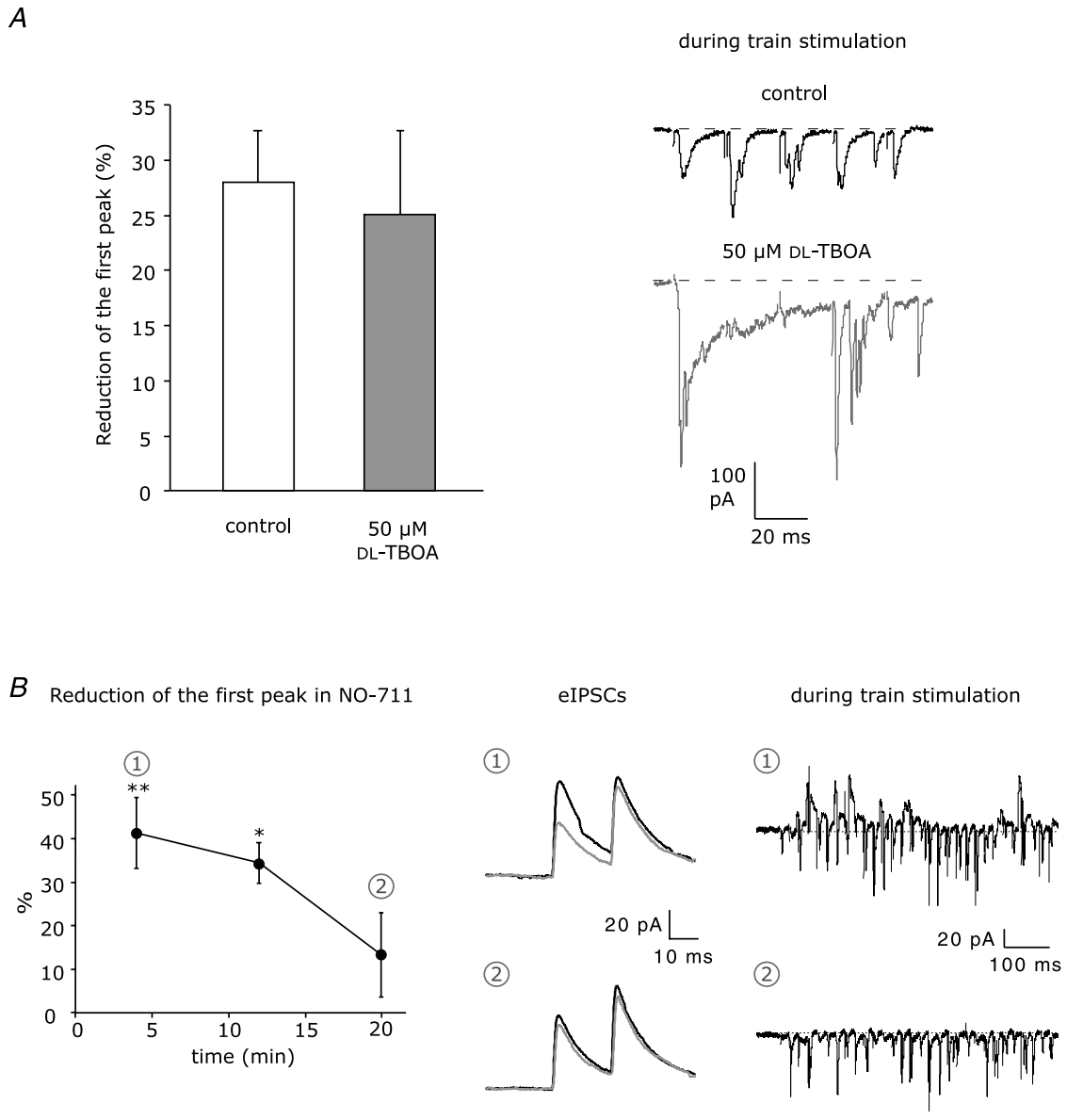

Figure 5. Blockade of glutamate and GABA transporters
A, left panel, train stimulation-induced disinhibition was tested in control ($n = 8$) and in the presence of the glutamate uptake inhibitor DL-TBOA (50 μM) and D-APV (50 μM) ($n = 8$). DL-TBOA did not enhance disinhibition, although glutamate spillover was promoted, as shown in the example traces on the right. *B*, blockade of GAT-1 by 5 μM NO-711 transiently enhanced train stimulation-induced disinhibition. On the left, reduction of eIPSCs is plotted against the recording time ($n = 6$). Each data point corresponds to the average of 16 responses. See Fig. 2*C* for statistical significance. In the middle, example eIPSCs from a single recording: average test responses (black) and conditioned responses (grey) in the first 8 min of recording (1) and after 20 min (2). On the right, example PSCs evoked during train stimulation during the first 8 min of recording (1) and after 20 min (2).

leads to an enhanced GABA-mediated tonic inhibition, we recorded the frequency of spontaneous spikes of stellate cells in the cell-attached configuration (see Methods). NO-711 at 5 μM reversibly decreased the spike frequency, indicating that NO-711 supported GABA-mediated tonic inhibition (control: 3.1 ± 0.7 Hz; NO-711, 5 μM: 1.0 ± 0.3 Hz, wash-out: 3.2 ± 0.9 Hz, $P < 0.05$, $n = 7$; Fig. 6*A*). Blockade of $GABA_A$Rs and $GABA_B$Rs with 10 μM SR-95531 (GABAzine) and 2 μM CGP-55845A, respectively, prevented NO-711-mediated

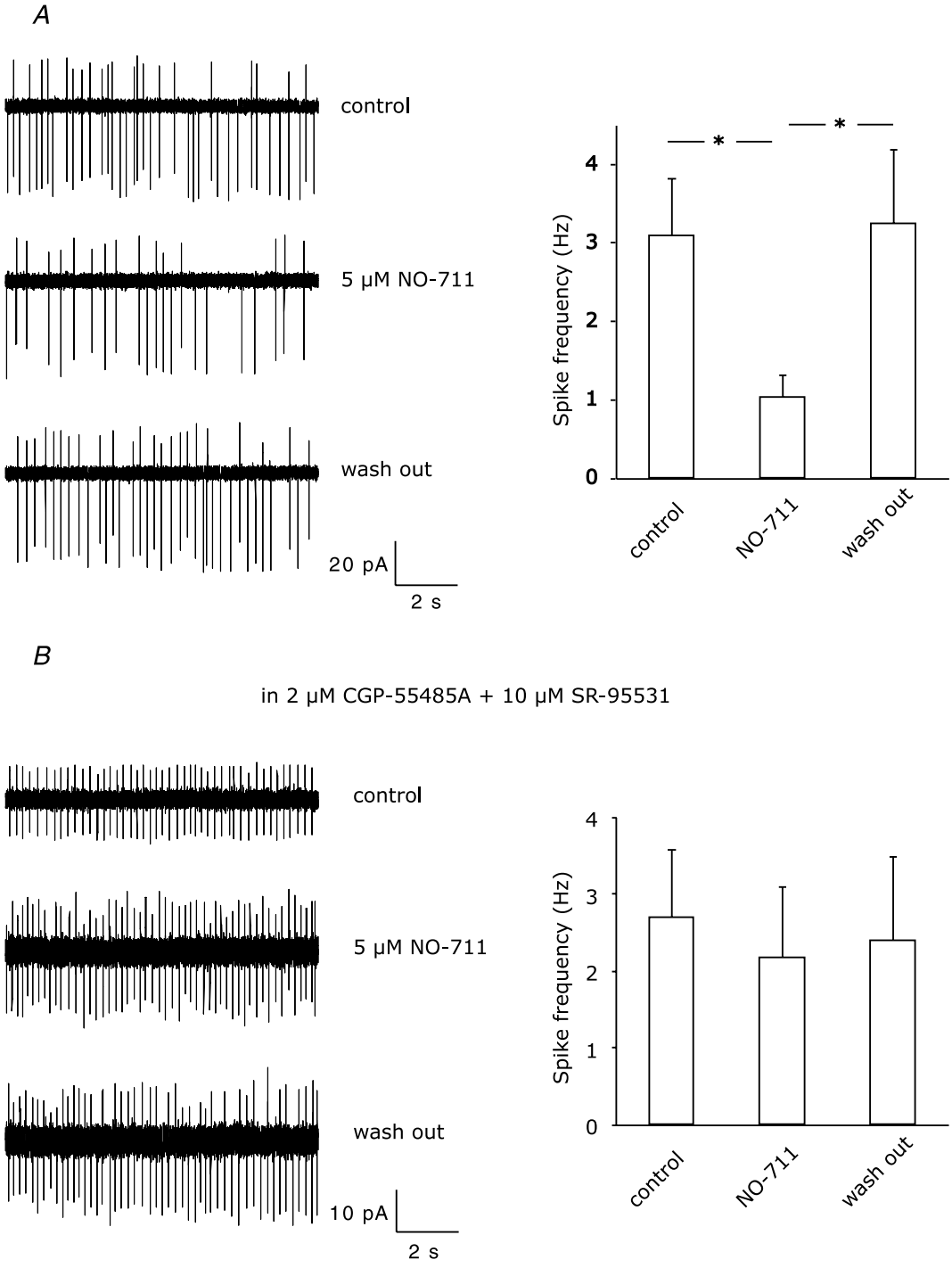

Figure 6. Effect of 5 μM NO-711 on spontaneous firing rate of stellate cells
A, on the left, example traces from a cell-attached recording showing reversible reduction of spike frequency. The summary of different recordings ($n = 7$) is depicted by the bars on the right. *B*, changes in spiking frequency were abolished by blockade of $GABA_B$ and $GABA_A$ receptors with 2 μM CGP-55845A and 10 μM SR-95531 ($n = 8$). Asterisks indicate statistical significance tested with paired Student's *t* test.

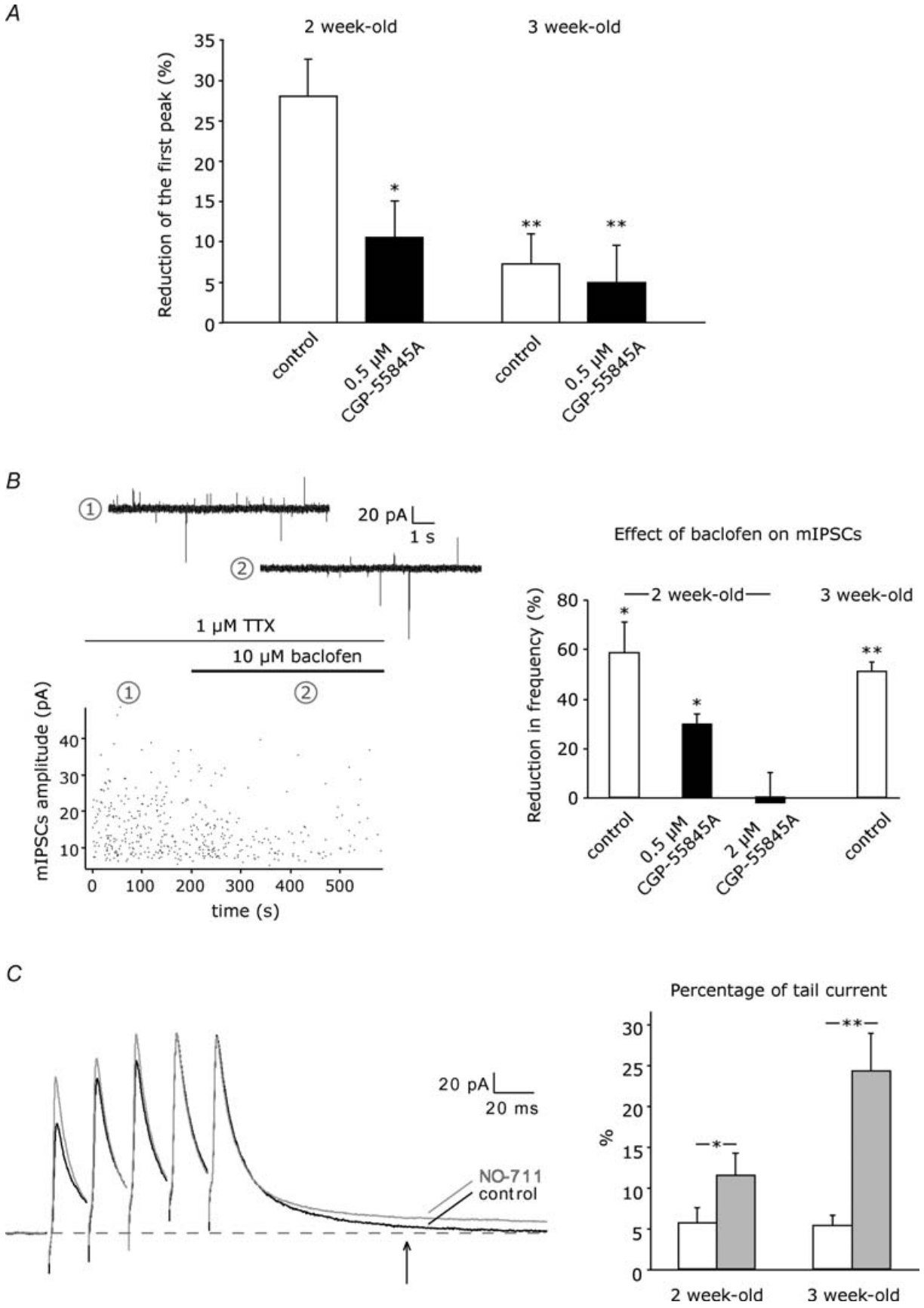

changes in firing frequency (control: 2.7 ± 0.9 Hz; NO-711, 5 μM: 2.2 ± 0.9 Hz, wash-out: 2.4 ± 1.1 Hz, $P > 0.05$, $n = 8$; Fig. 6*B*). Thus, enhanced tonic inhibition in the presence of GAT-1 blockers reduces firing of interneurons during train stimulation, thereby decreasing GABA release and spillover.

Developmental changes

We next examined disinhibition in 3-week-old mice with the protocol used in 2-week-old mice to compare the capability of presynaptic receptors to reduce GABA release in stellate cells at different postnatal stages. In slices of 3-week-old mice, train stimulation in the granule cell layer no longer induced significant disinhibition ($7.2 \pm 3.7\%$ reduction of eIPSCs, $P > 0.05$, $n = 10$; Fig. 7*A*).

The small disinhibitory effect in 3-week-old mice was not significantly affected by the high affinity $GABA_BR$ antagonist CGP-55845A (0.5 μM, $4.9 \pm 4.6\%$, $P > 0.05$, $n = 8$; Fig. 7*A*), although presynaptic $GABA_BRs$ are in 3-week-old mice as prominent as in 2-week-old mice. Superfusion of 10 μM baclofen, as was previously done in P7–17 guinea pigs (Mann-Metzer & Yarom, 2002), did not affect the peak amplitude but reduced the frequency of mIPSCs similarly at both ages (P14, $58.4 \pm 12.5\%$ frequency reduction, $P < 0.05$, $n = 5$; P21, $50.9 \pm 4.0\%$ frequency reduction, $P < 0.01$, $n = 6$; Fig. 7*B*), indicating that presynaptic $GABA_BRs$ are preserved at least until 3 weeks of age. At this point, we also tested the efficacy of CGP-55845A to prevent the baclofen-mediated frequency reduction of mIPSCs at P14 and found a dose dependency, in contrast to the paired recordings (Fig. 3). CGP-55845A at 0.5 μM reduced but at 2 μM completely blocked the baclofen effect (0.5 μM, $29.9 \pm 4.0\%$ frequency reduction, $P = 0.05$, $n = 4$; 2 μM, $-2.1 \pm 12.1\%$ frequency change, $P > 0.05$, $n = 5$, Fig. 7*B*). This efficacy difference was not observed during paired recordings (Fig. 3), when likely lower GABA concentrations were readily antagonized by 0.5 μM CGP-55845A in a competitive manner.

In addition, the reduced disinhibition in 3-week-old mice is also not explained by a developmental decrease in the probability of GABA release at stellate cell-to-stellate cell synapses, which could limit GABA spillover during train stimulation. For single stellate cell-to-stellate cell connections in 3-week-old mice, the paired-pulse ratio of eIPSCs was 1.05 ± 0.04, $n = 18$, and the average peak amplitude was 51.5 ± 6.2 pA, $n = 18$, i.e. not different from 2-week-old mice (P14, 0.96 ± 0.02, $n = 109$, $P > 0.05$; 56.6 ± 3.4 pA, $n = 109$, $P > 0.05$). Furthermore, the frequency of mIPSCs was actually higher in 3- compared to 2-week-old mice (P14, 0.9 ± 0.2 Hz, $n = 5$; P21, 3.8 ± 0.9 Hz, $n = 6$, $P < 0.05$; see also Bureau & Mulle (1998) for mIPSCs and sIPSCs), whereas the amplitude of mIPSCs was similar in 2- and in 3-week-old mice (P14, 16.1 ± 1.6 pA, $n = 5$; P21, 13.9 ± 1.6 pA, $n = 6$, $P > 0.05$). Thus, the probability of GABA release at stellate cell-to-stellate cell synapses does not strongly decrease between P14 and P21. This is in contrast to the > 10-fold developmental decrease in release probability observed at interneuron-to-Purkinje cell synapses in rats (Pouzat & Hestrin, 1997).

Lastly, we considered the possibility that the activation of presynaptic $GABA_BRs$ following the train stimulation is better controlled by GABA transporters in 3- than in 2-week-old mice. For this, we analysed tail currents present 100 ms after IPSC onset when evoked by train stimulation, e.g. five times at 50 Hz in the absence and the presence of a GAT-1 blocker (Fig. 7*C*). IPSCs were evoked by extracellular stimulation in the molecular layer in the presence of 50 μM GYKI-53655 and 50 μM D-APV. In the absence of GAT-1 blocker, the absolute tail currents were 5.9 ± 2.9 pA ($n = 6$) in 2-week-old and 4.6 ± 1.3 pA ($n = 6$) in 3-week-old mice, i.e. about 5% of the peak amplitude at both ages (Fig. 7*C*). In the presence of 5 μM NO-711, the tail currents increased at both ages (2-week-old mice, 11.9 ± 4.2 pA, $n = 6$; 3-week-old mice, 22.1 ± 6.2 pA, $n = 6$). This increase was more pronounced in 3-week-old mice, where the tail current was $24.3 \pm 4.6\%$ ($n = 6$) of the peak as compared to $11.5 \pm 2.7\%$ ($n = 6$) in 2-week-old mice (Fig. 7*C*). This indicates that in stellate cells of 3-week-old mice GABA transporters are either more prominent or more

Figure 7. Developmental changes
A, train stimulation-induced disinhibition was tested in 2- and 3-week-old mice in control ($n = 8$, $n = 10$, respectively) and in the presence of 0.5 μM CGP-55845A ($n = 8$, $n = 8$, respectively). See Fig. 3*A–C* for statistical significance. *B*, left panel, amplitude plot showing the effect of the $GABA_BR$ agonist baclofen (10 μM) on mIPSCs recorded from a stellate cell at a holding potential of −35 mV in a P14 mouse. Example traces represent recording in the absence (1) and in the presence (2) of baclofen. Right panel, summary data showing the reduction of mIPSCs frequency upon superfusion of 10 μM baclofen in 2- and 3-week-old mice (white bars, $n = 5$, $n = 6$, respectively). In 2-week-old mice, 2 μM CGP-55845A was needed to completely abolish the baclofen effect (black bars, 0.5 μM CGP: $n = 4$, 2 μM CGP: $n = 5$). See Fig. 2*C* for statistical significance. *C*, left panel, example recordings showing the effect on GAT-1 blockade (N0–711, 5 μM) on pharmacologically isolated eIPSCs evoked by a train stimulation (5 stimuli, 50 Hz) in the molecular layer of a P14 mouse. Average responses in NO-711 (grey) were normalized to control responses (black) relative to the fifth peak. Right panel, percentage tail current relative to peak amplitude was estimated at 100 ms after eIPSC onset in control (white bars) and in the presence of NO-711 (grey bars) in 2- and 3-week-old-mice ($n = 6$ for both age groups). Asterisks indicate statistical significance tested with paired Student's *t* test.

efficient than in 2-week-old mice, reducing the extent of presynaptic $GABA_BR$ activation which is required for disinhibition.

Discussion

The aim of the present study was to investigate the role of presynaptic receptors in modulating the evoked GABA release from cerebellar stellate cells when activated by endogenous neurotransmitter. Sustained excitatory input in the molecular layer generated by train stimulation in the granular layer disinhibited the stellate cell network. Peak amplitude of IPSCs elicited at unitary connections by firing of the presynaptic stellate cell was reduced by about 30%. This disinhibition could be more pronounced *in vivo*, when a larger number of parallel fibres is intact than in the sagittal slices used here for paired recordings. Maximal disinhibition occurred within tens of millisecond and diminished with time but remained significant up to 1 s. Consistently, prolonging the 50 Hz train stimulation from 600 to 1200 ms (30 *versus* 60 stimulations) induced a smaller disinhibitory effect.

Disinhibition at stellate cell-to-stellate cell synapses occurred via a presynaptic mechanism, i.e. reduction of GABA release from stellate cells, as indicated by concurrent increases in failure rate and coefficient of variation, in addition to a shift in the paired-pulse ratio towards facilitation. Consistently, peak amplitudes of axonal Ca^{2+} transients in identified Ca^{2+} hot spots (Forti *et al.* 2000) were reduced when preceded by a conditioning train stimulation that released glutamate in a region proximal to the interneuron axon. This effect is likely to be responsible for the reduced GABA release and strongly indicates that voltage-gated Ca^{2+} channels serve as the final target.

Stellate cells are known to express both AMPARs and $GABA_BRs$ also at presynaptic sites (Bureau & Mulle, 1998; Mann-Metzer & Yarom, 2002). Our experiments using application of agonists confirmed that both presynaptic AMPARs and $GABA_BRs$ are capable of modulating GABA release at stellate cell-to-stellate cell unitary connections. Superfusion of kainate or baclofen decreased peak amplitude of eIPSCs with concomitant increase of PPR, CV and failure rate. This agonist-mediated disinhibition recovered after perfusion of the respective antagonists. The baclofen-mediated effect was prevented by blockade of presynaptic G proteins, confirming the involvement of presynaptic metabotropic receptors.

Likewise, pharmacological dissection of the granule cell-mediated disinhibition indicated the involvement of AMPARs and $GABA_BRs$, whereas NMDARs, mGluRs and CB1 receptors could be excluded. Evidence for the involvement of presynaptic $GABA_BRs$ was provided by experiments using the high affinity antagonist CGP-55845A and by blockade of presynaptic G-proteins with GDPβ-S, which both strongly reduced disinhibition by two-thirds. The remaining disinhibitory effect when $GABA_BRs$ were blocked can be ascribed to presynaptic AMPARs, which in particular modulate autaptic currents in stellate cells (Liu, 2007). During the train stimulation, however, mainly postsynaptic AMPARs play a role by triggering the disynaptic pathway that leads to GABA release during the train stimulation, which explains the robust effect of AMPAR blockade on the disinhibition. Indeed, a substantial $GABA_BR$-mediated disinhibitory effect could be achieved by stimulating surrounding stellate cells in the molecular layer when AMPARs were blocked by GYKI-53655.

Glutamate released from parallel fibres during train stimulation and/or GABA released by excited surrounding interneurons could diffuse (spill over) to axon terminals of stellate cells to activate presynaptic receptors. Glutamate spillover is not essential under our experimental condition, since blockade of glutamate uptake by DL-TBOA, which should promote spillover, did not change the extent of disinhibition. This confirms that presynaptic AMPARs play a minor role, as discussed above. In contrast, GABA spillover was responsible for $GABA_BR$ activation, in a manner previously described between granule cells and Purkinje cells (Dittman & Regehr, 1997). Our attempt to directly demonstrate GABA spillover by blockade of GABA uptake using the GAT-1 blocker NO-711 was complicated by the initiation of two processes which are opposed to each other. As expected, blockade of GABA uptake increased tail currents during train stimulation and initially caused the disinhibitory effect to increase. On the other hand, blockade of GABA uptake leads to increased extracellular GABA concentration, which can cause presynaptic inhibition in many systems, including cerebellum (Rossi *et al.* 2003). Under our conditions, the reduced frequency of spontaneous spikes when blocking the GABA uptake was indicative of tonic inhibition. When tonically inhibited, stellate cells release less GABA during the train stimulation, and the consequential reduced GABA spillover explains why disinhibition was not enhanced in the continuous presence of the GAT-1 inhibitor.

The train stimulation-mediated disinhibition in the stellate cell network was developmentally regulated. Conditioned eIPSCs were significantly reduced in 2- but not in 3-week-old mice. This observation was surprising, since presynaptic $GABA_BRs$, in contrast to presynaptic AMPARs (Bureau & Mulle, 1998), do not undergo a developmental switch. When perfusing the $GABA_BR$ agonist baclofen, the frequency of mIPSCs similarly decreased at both developmental stages. Instead, limitations in GABA spillover in 3-week-old mice could explain the reduced disinhibition. Limitations in GABA spillover could arise from the possibility that GABA transporters are either more prominent or more efficient in 3-week-old mice, since blockade of GABA uptake

increased tail currents more prominently in 3- than in 2-week-old mice. Alternatively, limitations in GABA spillover could arise from a morphological change, i.e. from the reduced density of stellate cells in 3- compared with 2-week-old mice because of the about 1.5-fold increase of the thickness of the molecular layer (Yamanaka *et al.* 2004).

At the synapse between basket cell and Purkinje cell, activation of presynaptic AMPARs by endogenous glutamate reduced evoked GABA release (Satake *et al.* 2000). Therefore, our study reveals a clear difference between the two types of molecular layer interneurons. Strong excitatory inputs from parallel fibres modulate GABA release from stellate cells mainly via presynaptic $GABA_B$Rs through a disynaptic pathway, whereas disinhibition in basket cells can be induced by glutamate spillover from climbing fibres activating presynaptic AMPARs, without recruiting $GABA_B$Rs (Satake *et al.* 2004).

The negative regulation of inhibitory synapses triggered by excitatory inputs constitutes an example of cross talk between synapses, a phenomenon which takes place at various connections within the cerebellar circuitry (Dittman & Regehr, 1997; Rossi & Hamann, 1998; Satake *et al.* 2000; DiGregorio *et al.* 2002). Sustained glutamate release from parallel fibres has physiological relevance during perception, since it has been shown *in vivo* that somatosensory stimulation generates bursts of spikes in granule cells (Chadderton *et al.* 2004). Furthermore, *in vitro* studies have demonstrated that train stimulation protocols induce plasticity at excitatory synapses between parallel fibres and interneurons (Smith & Otis, 2005; Soler-Llavina & Sabatini, 2006). During the induction of plastic changes, disinhibition of GABAergic transmission could play an important role by modifying the balance between inhibitory and excitatory inputs in the molecular layer. Thus, the disinhibitory effect that acts within the network of GABAergic interneurons, with a temporal profile characteristic for short-term plasticity, could affect excitatory synapses between parallel fibres and interneurons over a longer time scale. The age dependence of the effect suggests that this mechanism could be critical in early postnatal stages when plastic changes are crucial for the refinement of synaptic connections and for the maturation of the cerebellar circuitry.

References

Biro AA & Nusser Z (2005). Synapse independence breaks down during highly synchronous network activity in the rat hippocampus. *Eur J Neurosci* **22**, 1257–1262.

Bureau I & Mulle C (1998). Potentiation of GABAergic synaptic transmission by AMPA receptors in mouse cerebellar stellate cells: changes during development. *J Physiol* **509**, 817–831.

Carter AG & Regehr WG (2000). Prolonged synaptic currents and glutamate spillover at the parallel fiber to stellate cell synapse. *J Neurosci* **20**, 4423–4434.

Chadderton P, Margrie TW & Hausser M (2004). Integration of quanta in cerebellar granule cells during sensory processing. *Nature* **428**, 856–860.

Clark BA & Cull-Candy SG (2002). Activity-dependent recruitment of extrasynaptic NMDA receptor activation at an AMPA receptor-only synapse. *J Neurosci* **22**, 4428–4436.

Diana MA & Bregestovski P (2005). Calcium and endocannabinoids in the modulation of inhibitory synaptic transmission. *Cell Calcium* **37**, 497–505.

Diana MA & Marty A (2003). Characterization of depolarization-induced suppression of inhibition using paired interneuron–Purkinje cell recordings. *J Neurosci* **23**, 5906–5918.

DiGregorio DA, Nusser Z & Silver RA (2002). Spillover of glutamate onto synaptic AMPA receptors enhances fast transmission at a cerebellar synapse. *Neuron* **35**, 521–533.

Dittman JS & Regehr WG (1997). Mechanism and kinetics of heterosynaptic depression at a cerebellar synapse. *J Neurosci* **17**, 9048–9059.

Dugue GP, Dumoulin A, Triller A & Dieudonne S (2005). Target-dependent use of co-released inhibitory transmitters at central synapses. *J Neurosci* **25**, 6490–6498.

Forti L, Pouzat C & Llano I (2000). Action potential-evoked Ca^{2+} signals and calcium channels in axons of developing rat cerebellar interneurones. *J Physiol* **527**, 33–48.

Glitsch M & Marty A (1999). Presynaptic effects of NMDA in cerebellar Purkinje cells and interneurons. *J Neurosci* **19**, 511–519.

Kondo S & Marty A (1998). Synaptic currents at individual connections among stellate cells in rat cerebellar slices. *J Physiol* **509**, 221–232.

Liu SJ (2007). Biphasic modulation of GABA release from stellate cells by glutamatergic receptor subtypes. *J Neurophysiol* **98**, 550–556.

Liu SJ & Lachamp P (2006). The activation of excitatory glutamate receptors evokes a long-lasting increase in the release of GABA from cerebellar stellate cells. *J Neurosci* **26**, 9332–9339.

Mann-Metzer P & Yarom Y (2002). Pre- and postsynaptic inhibition mediated by $GABA_B$ receptors in cerebellar inhibitory interneurons. *J Neurophysiol* **87**, 183–190.

Pouzat C & Hestrin S (1997). Developmental regulation of basket/stellate cell→Purkinje cell synapses in the cerebellum. *J Neurosci* **17**, 9104–9112.

Rossi DJ & Hamann M (1998). Spillover-mediated transmission at inhibitory synapses promoted by high affinity $\alpha 6$ subunit $GABA_A$ receptors and glomerular geometry. *Neuron* **20**, 783–795.

Rossi DJ, Hamann M & Attwell D (2003). Multiple modes of GABAergic inhibition of rat cerebellar granule cells. *J Physiol* **548**, 97–110.

Rusakov DA, Saitow F, Lehre KP & Konishi S (2005). Modulation of presynaptic Ca^{2+} entry by AMPA receptors at individual GABAergic synapses in the cerebellum. *J Neurosci* **25**, 4930–4940.

Satake S, Saitow F, Rusakov D & Konishi S (2004). AMPA receptor-mediated presynaptic inhibition at cerebellar GABAergic synapses: a characterization of molecular mechanisms. *Eur J Neurosci* **19**, 2464–2474.

Satake S, Saitow F, Yamada J & Konishi S (2000). Synaptic activation of AMPA receptors inhibits GABA release from cerebellar interneurons. *Nat Neurosci* **3**, 551–558.

Smith SL & Otis TS (2005). Pattern-dependent, simultaneous plasticity differentially transforms the input-output relationship of a feedforward circuit. *Proc Natl Acad Sci U S A* **102**, 14901–14906.

Soler-Llavina GJ & Sabatini BL (2006). Synapse-specific plasticity and compartmentalized signaling in cerebellar stellate cells. *Nat Neurosci* **9**, 798–806.

Takayama C & Inoue Y (2005). Developmental expression of GABA transporter-1 and 3 during formation of the GABAergic synapses in the mouse cerebellar cortex. *Brain Res Dev Brain Res* **158**, 41–49.

Yamanaka H, Yanagawa Y & Obata K (2004). Development of stellate and basket cells and their apoptosis in mouse cerebellar cortex. *Neurosci Res* **50**, 13–22.

Acknowledgements

We thank P. H. Seeburg for continuous support, G. Giese (W. Denk's Department) for support in two-photon microscopy, T. Kuner for an Igor macro to analyse miniature events, E. D'Angelo, A. Draguhn, U. Misgeld and I. Mody for helpful suggestions, and IVAX Drug Research Institute Ltd (Budapest, Hungary) for GYKI-53655. This work was supported by a Max-Planck fellowship to S.A. and the Deutsche Forschungsgemeinschaft Grant KO 1064/6.